Role of Inflammasome-independent Activation of IL-1β by the *Pseudomonas aeruginosa* Protease LasB

Running title: LasB Activation of IL-1β

Josh Sun[a], Doris L. LaRock[c], Elaine A. Skowronski[a], Jacqueline M. Kimmey[b,1], Joshua Olson[b], Zhenze Jiang[a], Anthony J. O'Donoghue[a], Victor Nizet[a,b], Christopher N. LaRock[c,d,e,#]

[a]Skaggs School of Pharmacy and Pharmaceutical Sciences, UC San Diego, La Jolla, CA, USA

[b]Department of Pediatrics, UC San Diego, La Jolla, CA, USA

[c]Department of Microbiology and Immunology, Emory School of Medicine, Atlanta GA, USA

[d]Division of Infectious Diseases, Emory School of Medicine, Atlanta GA, USA

[e]Antimicrobial Resistance Center, Emory University, Atlanta GA, USA

[#]Address correspondence to Christopher LaRock, christopher.larock@emory.edu

[1]Present address: Jacqueline Kimmey, Department of Microbiology and Environmental Toxicology, UC Santa Cruz, Santa Cruz, CA, USA

All authors declare no conflicts of interest

Abstract

Pulmonary damage by *Pseudomonas aeruginosa* during cystic fibrosis lung infection and ventilator-associated pneumonia is mediated both by pathogen virulence factors and host inflammation. Impaired immune function due to tissue damage and inflammation, coupled with pathogen multidrug resistance, complicates management of these deep-seated infections. Therefore, preservation of lung function and effective immune clearance may be enhanced by selectively controlling inflammation. Pathological inflammation during *P. aeruginosa* pneumonia is driven by interleukin-1β (IL-1β). This proinflammatory cytokine is canonically regulated by caspase-family inflammasome proteases, but we report that plasticity in IL-1β proteolytic activation allows for its direct maturation by the pseudomonal protease LasB. LasB promotes IL-1β activation, neutrophilic inflammation, and destruction of lung architecture characteristic of severe *P. aeruginosa* pulmonary infection. Discovery of this IL-1β regulatory mechanism provides a distinct target for anti-inflammatory therapeutics, such that matrix metalloprotease inhibitors blocking LasB limit inflammation and pathology during *P. aeruginosa* pulmonary infections.

Keywords: Pseudomonas aeruginosa; proteolysis; inflammation; lung;

Highlights:

- IL-1β drives pathology during pulmonary infection by *Pseudomonas aeruginosa*.
- The *Pseudomonas* protease LasB cleaves and activates IL-1β independent of canonical and noncanonical inflammasomes
- Metalloprotease inhibitors active against LasB limit inflammation and bacterial growth

Research in Context: Inflammation is highly damaging during lung infections by the opportunistic pathogen *Pseudomonas aeruginosa*. Sun et al. demonstrate that the *Pseudomonas* LasB protease directly activates IL-1β in an inflammasome-independent manner. Inhibition of IL-1β conversion by LasB protects against neutrophilic inflammation and destruction of the lung. Adjunctive therapeutics that limit pathological inflammation induced by infection would be beneficial for the treatment of pulmonary infections when used with conventional antibiotics.

Introduction

Pseudomonas aeruginosa is a prominent cause of severe opportunistic pulmonary infections associated with mechanical ventilation and the genetic disease cystic fibrosis (CF). *P. aeruginosa* infection is often refractory to antibiotic therapy due to multidrug resistance, making it a World Health Organization and U.S. Centers for Disease Control priority pathogen for therapeutic development. *P. aeruginosa* infection destroys lung architecture and function due to inflammatory- and neutrophil-mediated degradation of mucin layers and structural proteins of the pulmonary connective tissue [1,2]. Neutrophil cytokines such as IL-1β [3,4] and IL-8 [5], the latter itself regulated by IL-1β [6], initiate and maintain this inflammatory cycle. Anti-inflammatory agents can mitigate tissue destruction to preserve pulmonary function during *P. aeruginosa* pneumonia [7] and CF [8,9].

Newly synthesized IL-1β (pro-IL-1β) is inactive and requires proteolytic processing into a mature active form. Canonically, this is carried out by the inflammasome, a macromolecular complex of intracellular pattern recognition receptors and the proteases caspase-1 or caspase-11 [10]. During infection, inflammasomes are formed upon detection of pathogen-associated molecular patterns (PAMPs), including many present in *P. aeruginosa* such as flagellin (FliC), the type III secretion basal body rod (PscI), the type IV pilin (PilA), RhsT, exolysin (ExlA), exotoxin A (ExoA), cyclic 3′-5′ diguanylate (c-di-GMP), and lipopolysaccharide (LPS), which are varyingly detected by NLRC4, NLRP3, or caspase-11 [11-19]. Some pathogens limit inflammation by targeting the inflammasome [20], and *P. aeruginosa* dampens inflammasome activation via the effector ExoU [18]. Despite the multitude of inflammasome-activating signals that *P. aeruginosa* express, caspases, NLRP3, and NLRC4 are not essential for pro-IL-1β maturation in macrophages, epithelial cells, or neutrophils infected with *P. aeruginosa* [21,22]. Correspondingly, *P. aeruginosa*-infected caspase-$1^{-/-}$ and caspase-$1/11^{-/-}$ mice succumb to a destructive neutrophilic pulmonary inflammation against

which IL-1 receptor (IL-1R1$^{-/-}$) mice are protected [23]. These observations highlight the contribution of IL-1β to *P. aeruginosa* infection but suggest there are mechanisms for its maturation other than the inflammasome.

The pathological cascade of protease dysregulation and activation seen during severe *P. aeruginosa* lung infections provide a possibility for IL-1β maturation by alternative mechanisms. Caspase-8 [24-26], and the neutrophil granular proteases elastase (NE) and proteinase 3 (PR3) [3,4,27], cleave pro-IL-1β, but this does not always result in active cytokine [28]. Bronchial secretions, however, also possess abundant protease activity from microbial sources [2]. Here we find that IL-1β is not exclusively matured by host proteases, and that *P. aeruginosa* protease LasB also drives this inflammatory pathway. Targeting this bacterial protease may, therefore, provide supportive therapy to limit inflammatory pathology in pulmonary infection.

Results

IL-1β drives neutrophilic inflammation during *P. aeruginosa* lung infection

Inflammation drives poor clinical outcomes during *P. aeruginosa* lung infection [29]. C57Bl/6 mice infected intratracheally with *P. aeruginosa* had markedly disrupted airway architecture within 24 h, concurrent with neutrophil infiltration into the lung tissue and bronchoalveolar lavage fluid (BAL) (Figure 1A). We examined the contribution of pro-inflammatory cytokines to this process using the FDA-approved IL-1 receptor (IL-1R1) antagonist anakinra, which directly inhibits both IL-1β and IL-1α, but not other critical proinflammatory cytokines such as KC/CXCL1, IL-6, or TNFα (Figure 1B). As observed during human infections, *P. aeruginosa* persisted in the BAL (Figure 1C) and lung tissue (Figure 1D) despite significant neutrophil infiltration that was partially IL-1-dependent (Figure 1E).

IL-1β is typically released by secretion or cell lysis and requires additional maturation, activities which are all mediated by the inflammasome proteases caspases -1 or -11 [10]. CFU and release of IL-1α was unaltered in *P. aeruginosa*-infected caspase-1/11$^{-/-}$ C57Bl/6 mice, but surprisingly, IL-1β release was also only modestly attenuated (Figure 1F). This pool of extracellular IL-1β has the potential to mediate proinflammatory signaling as an IL-1R1 agonist when the inhibitory pro-domain has been removed. Neutrophil granular proteases may provide such activation [3,4,15,21], however, since neutrophil recruitment is itself IL-1β-dependent (Figure 1A, 1E), and these neutrophils themselves may later inactivate IL-1β [28], we reasoned that additional proteases initiate the process.

P. aeruginosa induces IL-1β maturation independent of the inflammasome

To more specifically measure only IL-1β that is active, we made use of transgenic reporter cells expressing luciferase under the control of the IL-1R (Figure 2A) similar to previously [30]. Consistent with our *in vivo* observations, caspase-1/11$^{-/-}$ bone-marrow-derived macrophages (BMM) still released cytokines that activated IL-1R1 reporter cells upon infection with *P. aeruginosa* PAO1 (Figure 2B). This activity was conserved across numerous *P. aeruginosa* isolates. In contrast, an ionophore that activates the NLRP3 inflammasome, nigericin, was completely dependent on caspases for the activation of IL-1 signaling. Furthermore, *P. aeruginosa* infection of human cell lines relevant to lung infection (macrophages, THP-1; neutrophils, HL60; type II alveolar epithelial cells, A549) still stimulated IL-1 signaling in the presence of the caspase-1/11-specific inhibitor YVAD-cmk (Figure 2C). Monoclonal antibodies specific to IL-1R1 or IL-1β, but not IL-1α, inhibited IL-1 signal from caspase-1/11$^{-/-}$ BMM (Figure 2D). The absolute

quantity of each cytokine measured by enzyme-linked immunosorbent assay (pro- and mature-forms) remained unchanged (Figure 2D). Together, these results indicate that *P. aeruginosa* stimulates IL-1 signaling through a pool of extracellular IL-1β that is active and matured independently of caspase-1/11.

IL-1β is activated by the *P. aeruginosa* LasB protease

Proteases contributing to IL-1β activation were evaluated using small molecule inhibitors specific to each protease class. Inhibition of metalloproteases, and not cysteine proteases (e.g. caspases-1, 11, and 8) or serine proteases (e.g. NE and PR3), abrogated IL-1β signaling in *P. aeruginosa*-infected caspase-1/11$^{-/-}$ BMM (Figure 3A). *P. aeruginosa* encodes several secreted metalloproteases, and by examining mutants of each (Δ*lasA*, Δ*lasB*, Δ*aprA*), we found LasB to be the most active protease overall as measured by hydrolysis of casein during agar plate growth (Figure 3B), and was the major contributor to caspase-1/11-independent IL-1β signaling (Figure 3C). Complementation with the LasB coding sequence under its native promoter restored the ability of Δ*lasB P. aeruginosa* to induce IL-1β signaling in infected caspase-1/11$^{-/-}$ BMM (Figure 3D). Furthermore, activation was independent of *il1b* expression (Figure 2E). These data show that LasB induces IL-1 signaling independently of caspase-1/11.

LasB-activated IL-1β is active

Incubation with recombinant LasB was sufficient to convert recombinant human pro-IL-1β into an active form (Figure 4A). Further examination of pro-IL-1β cleavage by LasB, again using recombinant forms of each protein, showed several intermediate cleavage products which accumulate as a stable product that is degraded no further (Figure 4B), similar to what occurs upon

IL-1β maturation by caspase-1 [31]. Analysis of these fragments by Edman sequencing identified cleavage sites that were all in the N-terminus of pro-IL-1β. Examination of N-terminal truncated IL-1β by *in vitro* transcription/translation showed a defined region flanking the caspase-1 cleavage site (N-term fragment 117) is sufficient to generate active cytokine (Figure 4C). We further examined proteolysis in this ~ 20 amino acid region with a series of internally quenched fluorescent peptides and found that LasB preferentially cleaved within the sequence HDAPVRSLN of pro-IL-1β (Figure 4D). Mass spectroscopy confirmed that LasB cleaved between Ser-121 and Leu-122 (Figure 4D, Figure S1), at a site conserved between mice and humans that matches the smallest IL-1β form we observed during SDS-PAGE (Figure 4B). This site also matches the substrate specificity profile for LasB (Figure 4E), which shows a distinct preference for cleaving peptide bonds when Ser or Thr are in the P1 position (amino-terminal side of bond) and hydrophobic amino acids such as Phe, Leu, Nle, Tyr, Trp and Ile in the P1′ position (Supplementary Spreadsheets 1-3), generated using a mass spectrometry-based substrate profiling assay previously validated with other microbial proteases [32,33]. During infection, the signature of IL-1β-targeted proteolysis (Figure 4F) is consistent with a significant role for LasB-mediated maturation (hydrolysis of HDAPVRSLN) compared to caspase-1 (hydrolysis of EAYVHDAPV) [30]. These data support the model that the pro-domain of IL-1β is promiscuous to protease activation and that the location of specific cleavages can dictate subsequent signaling activity.

Metalloprotease inhibitors of LasB prevent IL-1β -mediated pathological inflammation

Since IL-1β inhibition protects against lung damage (Figure 1A, 1B), and because LasB drives IL-1β maturation (Figure 3C, 4D), we examined whether protease inhibitors active against LasB limit lung injury. Two investigational hydroxamate-based anti-neoplastic metalloprotease inhibitors,

167 marimastat and ilomastat, inhibited LasB cleavage of the IL-1β-derived substrate (Figure 5A) and
168 *P. aeruginosa* activation of IL-1β (Figure 5B) at sub-antimicrobial concentrations (Figure S2A).
169 During murine pulmonary infection, marimastat and ilomastat each showed therapeutic effects to
170 reduce IL-1β (Figure 5C), neutrophil recruitment (Figure 5D), pulmonary pathology (Figure 5E),
171 and invasion (Figure S2B). Together this data suggests that inhibiting metalloproteases, including
172 LasB, can reduce inflammation during infections by *P. aeruginosa*.

173
174 **Discussion**

175 Opportunistic *P. aeruginosa* lung infections can destroy tissue structure and impair organ function.
176 Our findings reveal a mechanism by which a bacterial protease, LasB, contributes to pathological
177 inflammation by directly activating IL-1β. LasB is one of the most abundant virulence factors in
178 the lung microenvironment during *P. aeruginosa* infection and can cleave numerous host factors
179 [34], even exerting broadly anti-inflammatory influences through destructive proteolysis of PAMPs
180 such as flagellin [35], and various cytokines including IFN, IL-6, IL-8, MCP-1, TNF, trappin-2 and
181 RANTES [36-39]. Consequently, LasB-deficient bacteria may preferentially induce a KC, IL-6, and
182 IL-8 dominant inflammatory response [36], whereas we find wild-type *P. aeruginosa* induce a strong
183 IL-1β response.

184 LasB activates IL-1β through direct proteolytic removal of its inhibitory amino-terminal pro-
185 domain, bypassing the necessity for host caspases. The LasB and caspase-1 mechanisms for
186 generating mature IL-1β are distinguishable by substrate specificity (a hydrophobic P1' *vs* aspartic
187 acid P1 site), enzyme class (metalloprotease *vs* cysteine protease), and cellular source (microbial
188 *vs* host). LasB activation of pro-IL-1β in both the intra- and extracellular milieu is entirely feasible,
189 given the abundance of intracellular proteins released by pyroptosis and necrosis during infections

[10,40] and the abundance of LasB [41]. We recently hypothesized that IL-1β evolved as a sensor of diverse proteases [30], a model further supported by the present discovery of a *P. aeruginosa* protease with this activity.

In lung infection, LasB activation of IL-1β augments neutrophil recruitment and promotes destruction of the pulmonary tissue. IL-1β inhibition protects against this pathology, however, clinical interventions to date have utilized expensive biologics (e.g. IL-1R1 antagonists) associated with increased risk for severe infections [30,42]. The proteolytic activation of IL-1β may be a more tractable pharmacological target, made possible by disambiguation of the molecular networks involved and, perhaps amenable to the repurposing existing proteases inhibitors. Alpha-1-antitrypsin suppresses NE-mediated degradation of the CF lung [43,44], potentially also limiting pro-IL-1β maturation by NE [27]. This strategy may also act against pro-IL-1β maturation by LasB, which is also inhibited by alpha-1-antitrypsin [45]. Metalloprotease inhibitors such as marimastat and ilomastat may also be beneficial in treating CF [46] not only for inhibiting matrix metalloproteases, but also by cross-inhibiting LasB (Figure 5).

MATERIALS AND METHODS

Bacterial strains and plasmids. All bacterial strains, plasmids, and primers used in this study are listed in Table 1. *lasB* and the upstream 260 bp regulatory region in PAO1 were cloned into pUC18T-mini-Tn7T-*hph* [47] using Polymerase Incomplete Primer Extension (PIPE) cloning [48] with primers lasB-F, lasB-R, Tn7-F, and Tn7-R. Transformants into Top10 cells were selected on LB agar plates containing 100 µg/mL Hygromycin B (Life Technologies). Stable complementation into PAO1 Δ*lasB* was performed as previously described [47], and transformants selected with 400 µg/mL Hygromycin B. pET-LasB with a C-terminal His tag was constructed by sequential PIPE

cloning with the primers LasB-A, LasB-B, LasB-C, and LasB-D, and proteins were expressed and purified by conventional methods as previously described [30]. pET-pro-IL-1β and the purification of pro-IL-1β have been previously described [30]. Constructs for the expression of IL-1β mutants were generated by PIPE cloning from pET-pro-IL-1β [30] with the corresponding primers sets in Table 1, and proteins were expressed and purified in the same manner as for pro-IL-1β previously [30]. Bacteria were routinely propagated in Luria broth (LB) medium at 37 ºC. For infections, bacterial cultures were grown to late exponential phase (OD_{600} 1.2) then washed and diluted in PBS.

Animal Experiments. The UCSD or Emory University Institutional Animal Care and Use Committees approved all animal use. Eight-to-ten week old male or female C57Bl/6 and isogenic caspase-1/-11$^{-/-}$ mice were anesthetized with ketamine/xylazine intraperitoneally, then 10^7 CFU PAO1 inoculated intratracheally in 30 µl of 1x PBS, 25 µg/kg Ilomastat, and 25 µg/kg Marimastat. Mice were euthanized by CO_2 asphyxiation, and bronchiolar lavage fluid or lung homogenate were dilution plated onto LB agar plates for CFU enumeration, or quantification of cytokines or proteolysis. Bronchiolar lavage fluid cells were counted on a hemocytometer with cytologic examination on cytospin preparations fixed and stained using Hema 3 (Fisher HealthCare™). Histologic sections were prepared from formalin-fixed and paraffin-embedded lungs, stained with hematoxylin and eosin (H&E). Cytospin and histology slides were imaged on a Hamamatsu Nanozoomer 2.0Ht Slide Scanner.

***In vitro* infection models.** Macrophages were generated from femur exudates of wild-type C57Bl/6 (Jackson Laboratories) or caspase-1/11$^{-/-}$ (kindly provided by R. Flavell) mice using M-CSF containing L929 cell supernatants as previously [30]. THP-1, HL60, and A549 cells were propagated by standard protocols detailed previously [49]. One hour before infection, the media was

replaced with RPMI lacking phenol red, fetal bovine serum, and antibiotics. Inhibitor treatments were added 1 h before infection and include: 20 μg/mL Anakinra (Amgen), 100 ng/mL rIL-1β (R&D Systems), 5 μM caspase inhibitors zVAD-fmk, YVAD-fmk, DEVD-fmk, and IETD-fmk (R&D Systems), 10 μg/mL complete protease inhibitor cocktail (Roche), 1x protease inhibitors AEBSF, Antipain, Aprotinin, Bestatin, EDTA, E-64, Phosphoramidon, Pepstatin, and PMSF (G-Biosciences). Except when noted, cells were routinely infected by co-incubation with *P. aeruginosa* at a multiplicity of infection of 10, spun into contact for 3 min at 300 g, and cells or supernatants were harvested for analysis after 2 h.

Cytokine measurements. Relative IL-1 signaling by cells was measured in 50 μl of supernatant from infected or treated cells, then incubated with 1 μM okadaic acid 30 min before transfer onto transgenic IL-1R reporter cells (Invivogen). After 18 h, reporter cell supernatants were analyzed for secreted alkaline phosphatase activity using HEK-Blue Detection reagent (Invivogen). Cytokines were quantified by enzyme-linked immunosorbent assay following the manufacturer's protocol (R&D Systems). Expression was examined in cells lysed with RIPA (Millipore). RNA was isolated (Qiagen), cDNA synthesized with SuperScript III and Oligo(dT)20 primers (Invitrogen), and qPCR performed with KAPA SYBR Fast (Kapa Biosystems) with primers for *il1b* and relative expression normalized to *gapdh* and compared by ΔΔCt as previously [50]. *In vitro* transcription/translation was performed with the corresponding primers in **Table 1** using pET-pro-IL-1β as a template and following the manufacturer's recommendations in 10 μl reaction volumes (TNT Coupled Reticulocyte Lysate; Promega). Loading for IL-1R reporter assays was normalized by total IL-1β product measured by enzyme-linked immunosorbent assay (R&D Systems).

Substrate specificity profiling. 10 nM LasB was incubated in triplicate with a mixture of 228 synthetic tetradecapeptides (0.5 μM each) in PBS, 2mM DTT as described previously [51]. After 15,

60, 240 and 1200 min, aliquots were removed, quenched with 6.4 M GuHCl, immediately frozen at -80°C. Controls were performed with LasB treated with GuHCl prior to peptide exposure. Samples were acidified to pH<3.0 with 1% formic acid, desalted with C18 LTS tips (Rainin), and injected into a Q-Exactive Mass Spectrometer (Thermo) equipped with an Ultimate 3000 HPLC. Peptides separated by reverse phase chromatography on a C18 column (1.7 µm bead size, 75 µm x 20 cm, 65°C) at a flow rate of 400 nl/min using a linear gradient from 5% to 30% B, with solvent A: 0.1% formic acid in water and solvent B: 0.1% formic acid in acetonitrile. Survey scans were recorded over a 150–2000 m/z range (70000 resolutions at 200 m/z, AGC target 1×10^6, 75 ms maximum). MS/MS was performed in data-dependent acquisition mode with HCD fragmentation (30 normalized collision energy) on the 10 most intense precursor ions (17500 resolutions at 200 m/z, AGC target 5×10^4, 120 ms maximum, dynamic exclusion 15 s).

Peak integration and data analysis were performed using Peaks software (Bioinformatics Solutions Inc.). MS^2 data were searched against the tetradecapeptide library sequences and a decoy search was conducted with sequences in reverse order with no protease digestion specified. Data were filtered to 1% peptide and protein level false discovery rates with the target-decoy strategy. Peptides were quantified with label free quantification and data normalized by LOWESS and filtered by 0.3 peptide quality. Missing and zero values are imputed with random normally distributed numbers in the range of the average of smallest 5% of the data±SD. Enzymatic progress curves of each unique peptide were obtained by performing nonlinear least-squares regression on their peak areas in the MS precursor scans using the first-order enzymatic kinetics model: $Y = (\text{plateau}-Y_0)\times(1-\exp(-t\times k_{cat}/K_M\times[E_0]))+Y_0$, where E_0 is the total enzyme concentration. Nonlinear regression was performed on cleavage products only if the following criteria were met: Peptides were detected in at least 2 of the 3 replicates and the peak intensity of peptides increased by

281 >50,000 and >5-fold over the course of the assay. Proteolytic efficiency was solved from the
282 progress curves by estimating total enzyme concentration and is reported as k_{cat}/K_M and clustered
283 into 8 groups by Jenks optimization method. IceLogo software was used for visualization of
284 amino-acid frequency using cleavage sequences in the top 3 clusters (118 most efficiently cleaved
285 peptides). Mass spectrometry deposited: ftp://massive.ucsd.edu/MSV000081623.

286 **Protease Measurements**. Internally-quenched peptides 7-Methoxycoumarin- (Mca) labeled on
287 the amino terminus and 2, 4-dinitrophenyl (Dnp) on the carboxy terminus were synthesized with
288 the sequences of IFFDTWDNE, TWDNEAYVH, EAYVHDAPV, and HDAPVRSLN,
289 corresponding to amino acids 103-111, 107-115, 111-119, and 115-123 of the reference human
290 pro-IL-1β sequence (UniProt: P01584; CPC Scientific). In triplicate, 10 μM peptides were
291 incubated in PBS, 1 mM $CaCl_2$, 0.01% Tween-20, with 5 nM human caspase-1 (Enzo) or LasB
292 (Elastin Products Co.). The reaction was continuously monitored using an EnSpire plate reader
293 (PerkinElmer) with 323nm fluorophore excitation and 398nm emission and the maximum kinetic
294 velocity calculated as previously [30]. The cleavage site was determined by incubating 10 nM of
295 LasB with 10 μM of HDAPVRSLN. At 20, 40 and 60 min intervals each reaction was quenched
296 with 6.4 M GuHCl and the cleavage products desalted and analyzed by mass spectrometry as
297 described above, except using a 20-min linear gradient from 5% to 50% B and only selecting top
298 5 peptides for MS/MS.

299 **Statistical analysis**. Statistical significance was calculated by unpaired Student t test (*, $P < 0.05$;
300 **, $P < 0.005$) using GraphPad Prism unless otherwise indicated. Data are representative of at least
301 three independent experiments. For iceLogo plots only amino acids with significantly ($P < 0.05$)
302 increased or decreased frequency are shown.

303
304 **Acknowledgments**

We thank Christopher Lietz (UCSD) for assistance with mass spectrometry and data analysis, the UCSD Histopathology Core facility, the UCSD Neuroscience Microscopy Shared Facility (P30 NS047101), Jason Munguia (UCSD) for technical assistance, Colin Manoil (UW) for *Pseudomonas* transposon mutants (P30 DK089507) and Joanna Goldberg (Emory) for helpful advice and discussions. J.S. received support from NIH/NIGMS T32 GM007752, E.A.S. from NIH/NCI T32 CA121938, J.M.K. from a UC President's Postdoctoral Fellowship, Z.J. from the UC San Diego Chancellor's Research Excellence Scholarship, A.J.O. from NIH/NIBIB AI1333393, V.N. from NIH/NICHD grant U54 HD090259 and NIH/NHLBI R01 HL125352, and C.L. the A.P. Giannini Foundation and NIH/NIAID K22 AI130223. C.N.L. has a research agreement with Antabio examining inhibitors of LasB. The content is solely the responsibility of the authors and does not necessarily represent the official views of the National Institutes of Health.

Author contributions

J.S., A.J.O., V.N., and C.N.L. designed experiments and interpreted the data. J.S., D.L., J.K., J.O., Z.J., E.A.S., A.J.O., and C.N.L conducted the studies. J.S., V.N., and C.N.L. wrote the manuscript with the assistance of all of the authors.

References

1. Suter S, Schaad UB, Roux L, Nydegger UE, Waldvogel FA. Granulocyte neutral proteases and Pseudomonas elastase as possible causes of airway damage in patients with cystic fibrosis. *Journal of Infectious Diseases* 1984; **149**(4): 523-31.

2. Twigg MS, Brockbank S, Lowry P, FitzGerald SP, Taggart C, Weldon S. The role of serine proteases and antiproteases in the cystic fibrosis lung. *Mediators of inflammation* 2015; **2015**: 293053.

3. Coeshott C, Ohnemus C, Pilyavskaya A, et al. Converting enzyme-independent release of tumor necrosis factor α and IL-1β from a stimulated human monocytic cell line in the presence of activated neutrophils or purified proteinase 3. *Proceedings of the National Academy of Sciences of the United States of America* 1999; **96**: 6261-6.

4. Greten FR, Arkan MC, Bollrath J, et al. NF-κB is a negative regulator of IL-1β secretion as revealed by genetic and pharmacological inhibition of IKKβ. *Cell* 2007; **130**(5): 918-31.

5. Nakamura H, Yoshimura K, McElvaney NG, Crystal RG. Neutrophil elastase in respiratory epithelial lining fluid of individuals with cystic fibrosis induces interleukin-8 gene expression in a human bronchial epithelial cell line. *Journal of Clinical Investigation* 1992; **89**(5): 1478.

6. Labrousse D, Perret M, Hayez D, et al. Kineret®/IL-1ra Blocks the IL-1/IL-8 Inflammatory Cascade during Recombinant Panton Valentine Leukocidin-Triggered Pneumonia but Not during S. aureus Infection. *PloS one* 2014; **9**(6): e97546.

7. Schultz MJ, Rijneveld AW, Florquin S, Edwards CK, Dinarello CA, van der Poll T. Role of interleukin-1 in the pulmonary immune response duringPseudomonas aeruginosa pneumonia. *American Journal of Physiology-Lung Cellular and Molecular Physiology* 2002; **282**(2): L285-L90.

8. Fritzsching B, Zhou-Suckow Z, Trojanek JB, et al. Hypoxic Epithelial Necrosis Triggers Neutrophilic Inflammation via IL-1 Receptor Signaling in Cystic Fibrosis Lung Disease. *American journal of respiratory and critical care medicine* 2015; **191**(8): 902-13.

9. Konstan MW, Byard PJ, Hoppel CL, Davis PB. Effect of high-dose ibuprofen in patients with cystic fibrosis. *New England Journal of Medicine* 1995; **332**(13): 848-54.

10. LaRock CN, Cookson BT. Burning down the house: cellular actions during pyroptosis. *PLoS pathogens* 2013; **9**(12): e1003793.

11. Abdul-Sater AA, Tattoli I, Jin L, et al. Cyclic-di-GMP and cyclic-di-AMP activate the NLRP3 inflammasome. *EMBO reports* 2013; **14**(10): 900-6.

12. Lindestam Arlehamn CS, Evans TJ. Pseudomonas aeruginosa pilin activates the inflammasome. *Cellular microbiology* 2011; **13**(3): 388-401.

13. Basso P, Ragno M, Elsen S, et al. Pseudomonas aeruginosa pore-forming exolysin and Type IV Pili Cooperate to induce host cell lysis. *MBio* 2017; **8**(1): e02250-16.

14. Franchi L, Stoolman J, Kanneganti TD, Verma A, Ramphal R, Núñez G. Critical role for Ipaf in *Pseudomonas aeruginosa*-induced caspase-1 activation. *European journal of immunology* 2007; **37**(11): 3030-9.

15. Lin AE, Beasley FC, Keller N, et al. A Group A Streptococcus ADP-Ribosyltransferase Toxin Stimulates a Protective Interleukin 1β-Dependent Macrophage Immune Response. *mBio* 2015; **6**(2): e00133-15.

16. Miao EA, Ernst RK, Dors M, Mao DP, Aderem A. *Pseudomonas aeruginosa* activates caspase 1 through Ipaf. *Proceedings of the National Academy of Sciences* 2008; **105**(7): 2562-7.

17. Miao EA, Mao DP, Yudkovsky N, et al. Innate immune detection of the type III secretion apparatus through the NLRC4 inflammasome. *Proceedings of the National Academy of Sciences of the United States of America* 2010; **107**(7): 3076-80.

18. Sutterwala FS, Mijares LA, Li L, Ogura Y, Kazmierczak BI, Flavell RA. Immune recognition of *Pseudomonas aeruginosa* mediated by the IPAF/NLRC4 inflammasome. *The Journal of Experimental Medicine* 2007; **204**(13): 3235-45.

19. Kung VL, Khare S, Stehlik C, Bacon EM, Hughes AJ, Hauser AR. An *rhs* gene of *Pseudomonas aeruginosa* encodes a virulence protein that activates the inflammasome. *Proceedings of the National Academy of Sciences* 2012; **109**(4): 1275-80.

20. LaRock CN, Cookson BT. The Yersinia Virulence Effector YopM Binds Caspase-1 to Arrest Inflammasome Assembly and Processing. *Cell Host & Microbe* 2012; **12**(6): 799-805.

21. Karmakar M, Sun Y, Hise AG, Rietsch A, Pearlman E. Cutting edge: IL-1β processing during Pseudomonas aeruginosa infection is mediated by neutrophil serine proteases and is independent of NLRC4 and caspase-1. *The Journal of Immunology* 2012; **189**(9): 4231-5.

22. Anantharajah A, Buyck JM, Faure E, et al. Correlation between cytotoxicity induced by Pseudomonas aeruginosa clinical isolates from acute infections and IL-1β secretion in a model of human THP-1 monocytes. *Pathogens and disease* 2015; **73**(7): ftv049.

23. Al Moussawi K, Kazmierczak BI. Distinct Contributions of Interleukin-1α (IL-1α) and IL-1β to Innate Immune Recognition of Pseudomonas aeruginosa in the Lung. *Infection and Immunity* 2014; **82**(10): 4204-11.

24. Ganesan S, Rathinam VAK, Bossaller L, et al. Caspase-8 modulates dectin-1 and complement receptor 3-driven IL-1beta production in response to beta-glucans and the fungal pathogen, Candida albicans. *J Immunol* 2014; **193**(5): 2519-30.

25. Maelfait J, Vercammen E, Janssens S, et al. Stimulation of Toll-like receptor 3 and 4 induces interleukin-1beta maturation by caspase-8. *J Exp Med* 2008; **205**(9): 1967-73.

26. Van Opdenbosch N, Van Gorp H, Verdonckt M, et al. Caspase-1 Engagement and TLR-Induced c-FLIP Expression Suppress ASC/Caspase-8-Dependent Apoptosis by Inflammasome Sensors NLRP1b and NLRC4. *Cell reports* 2017; **21**(12): 3427-44.

27. Hsu L-C, Enzler T, Seita J, et al. IL-1 [beta]-driven neutrophilia preserves antibacterial defense in the absence of the kinase IKK [beta]. *Nature immunology* 2011; **12**(2): 144-50.

28. Clancy DM, Sullivan GP, Moran HBT, et al. Extracellular Neutrophil Proteases Are Efficient Regulators of IL-1, IL-33, and IL-36 Cytokine Activity but Poor Effectors of Microbial Killing. *Cell Reports* 2018; **22**(11): 2937-50.

29. Conese M, Copreni E, Di Gioia S, De Rinaldis P, Fumarulo R. Neutrophil recruitment and airway epithelial cell involvement in chronic cystic fibrosis lung disease. *Journal of Cystic fibrosis* 2003; **2**(3): 129-35.

30. LaRock CN, Todd J, LaRock D, et al. IL-1β is an innate immune sensor of microbial proteolysis. *Science Immunology* 2016; **1**(2).

31. Howard AD, Kostura MJ, Thornberry N, et al. IL-1-converting enzyme requires aspartic acid residues for processing of the IL-1 beta precursor at two distinct sites and does not cleave 31-kDa IL-1 alpha. *The Journal of Immunology* 1991; **147**(9): 2964.

32. Lapek JD, Jr., Jiang Z, Wozniak JM, et al. Quantitative Multiplex Substrate Profiling of Peptidases by Mass Spectrometry. *Mol Cell Proteomics* 2019; **18**(5): 968-81.

33. Xu JH, Jiang Z, Solania A, et al. A Commensal Dipeptidyl Aminopeptidase with Specificity for N-Terminal Glycine Degrades Human-Produced Antimicrobial Peptides in Vitro. *ACS Chem Biol* 2018; **13**(9): 2513-21.

34. Beaufort N, Corvazier E, Mlanaoindrou S, de Bentzmann S, Pidard D. Disruption of the endothelial barrier by proteases from the bacterial pathogen Pseudomonas aeruginosa: implication of matrilysis and receptor cleavage. *PLoS One* 2013; **8**(9): e75708.

35. Casilag F, Lorenz A, Krueger J, Klawonn F, Weiss S, Häussler S. The LasB elastase of Pseudomonas aeruginosa acts in concert with alkaline protease AprA to prevent flagellin-mediated immune recognition. *Infection and immunity* 2016; **84**(1): 162-71.

36. LaFayette SL, Houle D, Beaudoin T, et al. Cystic fibrosis–adapted Pseudomonas aeruginosa quorum sensing lasR mutants cause hyperinflammatory responses. *Science advances* 2015; **1**(6): e1500199.

37. Matheson NR, Potempa J, Travis J. Interaction of a novel form of Pseudomonas aeruginosa alkaline protease (aeruginolysin) with interleukin-6 and interleukin-8. *Biological chemistry* 2006; **387**(7): 911-5.

38. Parmely M, Gale A, Clabaugh M, Horvat R, Zhou WW. Proteolytic inactivation of cytokines by Pseudomonas aeruginosa. *Infection and Immunity* 1990; **58**(9): 3009-14.

427 39. Saint-Criq V, Villeret B, Bastaert F, et al. Pseudomonas aeruginosa LasB protease
428 impairs innate immunity in mice and humans by targeting a lung epithelial cystic fibrosis
429 transmembrane regulator–IL-6–antimicrobial–repair pathway. *Thorax* 2017: thoraxjnl-2017-
430 210298.

431 40. Afonina IS, Müller C, Martin SJ, Beyaert R. Proteolytic processing of interleukin-1
432 family cytokines: variations on a common theme. *Immunity* 2015; **42**(6): 991-1004.

433 41. Jaffar-Bandjee MC, Lazdunski A, Bally M, Carrère J, Chazalette JP, Galabert C.
434 Production of elastase, exotoxin A, and alkaline protease in sputa during pulmonary exacerbation
435 of cystic fibrosis in patients chronically infected by Pseudomonas aeruginosa. *Journal of Clinical*
436 *Microbiology* 1995; **33**(4): 924-9.

437 42. Cabral VP, Andrade CAFd, Passos SRL, Martins MdFM, Hökerberg YHM. Severe
438 infection in patients with rheumatoid arthritis taking anakinra, rituximab, or abatacept: A
439 systematic review of observational studies. *Revista brasileira de reumatologia* 2016; **56**(6): 543-
440 50.

441 43. Cantin AM, Woods DE. Aerosolized prolastin suppresses bacterial proliferation in a
442 model of chronic Pseudomonas aeruginosa lung infection. *American journal of respiratory and*
443 *critical care medicine* 1999; **160**(4): 1130-5.

444 44. Martin SL, Downey D, Bilton D, Keogan MT, Edgar J, Elborn JS. Safety and Efficacy of
445 Recombinant Alpha1-Antitrypsin Therapy in Cystic Fibrosis. *Pediatric pulmonology* 2006;
446 **41**(2): 177-83.

447 45. O'Connor CM, Gaffney K, Keane J, et al. ~ 1-Proteinase Inhibitor, Elastase Activity, and
448 Lung Disease Severity in Cystic Fibrosis. *American Review of Respiratory Disease* 1993; **148**:
449 1665-.

450 46. Gaggar A, Hector A, Bratcher PE, Mall MA, Griese M, Hartl D. The role of matrix
451 metalloproteinases in cystic fibrosis lung disease. *European Respiratory Journal* 2011; **38**(3):
452 721-7.

453 47. Choi KH, Schweizer HP. mini-Tn7 insertion in bacteria with single attTn7 sites: example
454 Pseudomonas aeruginosa. *Nature Protocols* 2006; **1**(1): 153.

455 48. Klock HE, Lesley SA. The Polymerase Incomplete Primer Extension (PIPE) method
456 applied to high-throughput cloning and site-directed mutagenesis. *High Throughput Protein*
457 *Expression and Purification: Methods and Protocols* 2009: 91-103.

458 49. LaRock CN, Döhrmann S, Todd J, et al. Group A Streptococcal M1 Protein Sequesters
459 Cathelicidin to Evade Innate Immune Killing. *Cell host & microbe* 2015; **18**(4): 1-7.

460 50. LaRock DL, Sands JS, Ettouati E, et al. Inflammasome inhibition blocks cardiac
461 glycoside cell toxicity. *Journal of Biological Chemistry* 2019; **294**(34): 12846-54.

462 51. O'Donoghue AJ, Knudsen GM, Beekman C, et al. Destructin-1 is a collagen-degrading
463 endopeptidase secreted by Pseudogymnoascus destructans, the causative agent of white-nose
464 syndrome. *Proceedings of the National Academy of Sciences* 2015; **112**(24): 7478-83.

465 52. Jacobs MA, Alwood A, Thaipisuttikul I, et al. Comprehensive transposon mutant library
466 of Pseudomonas aeruginosa. *Proceedings of the National Academy of Sciences* 2003; **100**(24):
467 14339-44.
468
469

FIGURE LEGENDS

Figure 1. IL-1β drives neutrophilic inflammation during *P. aeruginosa* lung infection

C57BL/6 mice intratracheally infected with 10^7 colony forming units (CFU) of PAO1 and treated with anakinra (50 μg/kg) or PBS control, compared to uninfected mice. Mice were euthanized after 24 h and (**A**) lung histology sections or cytological smears of bronchoalveolar lavage fluid (BAL) prepared with differential MGG stain, (**B**) BAL cytokines measured by enzyme-linked immunosorbent assay, (**C-D**) bacterial CFU in BAL or lung homogenate, and (**E**) BAL neutrophils enumerated. (**F**) C57BL/6 or isogeneic caspase-1/11$^{-/-}$ mice intratracheally infected with 10^7 CFU PAO1 24 h, euthanized, and BAL cytokines measured by enzyme-linked immunosorbent assay. Where applicable, data are mean ± SEM and represent at least 3 independent experiments. Significance determined by Mann-Whitney U-test (*$P < 0.05$, **$P < 0.005$).

Figure 2. *P. aeruginosa* induces IL-1β maturation independent of the inflammasome

(**A**) Diagram of IL-1 reporter assay. Pro-IL-1β does not induce signaling through the IL-1R. Removal of the pro-domain, intracellularly or extracellularly, by any protease that can do so, results in an active cytokine with proinflammatory activity. (**B**) Relative IL-1 signaling by caspase-1/11$^{-/-}$ (grey) or control C57Bl/6 BMMs (black) after 2 h co-incubation of the indicated *Pseudomonas* strains. Nigericin (5 μM) is included as a positive control for inflammasome-dependent IL-1β maturation. (**C**) Mature IL-1 and enzyme-linked immunosorbent assay measurement of IL-1α and IL-1β present in any form, released from PAO1-infected caspase-1/11$^{-/-}$ BMM with monoclonal antibodies neutralizing IL-1R1, IL-1α, IL-1β, or an isotype control. (**D**) Relative IL-1 signaling by human THP-1 macrophages, HL60 neutrophils, or A549 epithelial cells treated with caspase-1 inhibitor (YVAD) or control (Mock) 1 h prior to infection. Infections were

493 at MOI=10 and after 2 h the supernatant collected and mature IL-1 quantified using IL-1R1
494 reporter cells. Where applicable, data are mean ± SEM and represent at least 3 independent
495 experiments; significance determined by unpaired two-tailed Student's T-test, *$P < 0.05$.
496
497 **Figure 3. IL-1β is activated by the *P. aeruginosa* LasB protease**
498 (**A**) Relative IL-1 signaling by caspase-1/11$^{-/-}$ BMM 2 h post-infection by PAO1 that were
499 previously incubated 1 h with the indicated protease inhibitors classes. (**B**) Visualization of
500 bacterial proteolytic activity by decreased media opacity on LB agarose plates containing casein.
501 (**C**) Relative IL-1 signaling by caspase-1/11$^{-/-}$ BMM 2 h post-infection with isogenic mutant strains
502 of PAO1. (**D**) Relative IL-1 signaling by caspase-1/11$^{-/-}$ BMM 2 h post-infection by PAO1, Δ*lasB*,
503 or plasmid-complemented Δ*lasB* and (**E**) *il1b* expression by real-time quantitative PCR. Where
504 applicable, data are mean ± SEM and represent at least 3 independent experiments; significance
505 determined by unpaired two-tailed Student's T-test, *$P < 0.05$.
506
507 **Figure 4. LasB-activated IL-1β is active**
508 (**A**) IL-1 signaling activity by human pro-IL-1β after 2 h incubation with titrations of recombinant
509 LasB. **(B**) SDS-PAGE analysis of recombinant human pro-IL-1β maturation by recombinant LasB.
510 **(C**) Signaling activity of recombinant IL-1β N-terminal truncations generated using *in vitro*
511 transcription/translation from each codon, 1 is full-length pro-IL-1β, 117 corresponds to the
512 fragment generated by caspase-1 cleavage. **(D**) Cleavage of internally-quenched fluorescent IL-1β
513 peptide fragments (amino acids 103-123 of human IL-1β) by recombinant LasB or caspase-1. (**E**)
514 IceLogo frequency plot showing amino acids significantly enriched (above X-axis) and de-
515 enriched (below X-axis) in the P2 to P2′ positions following incubation of LasB with a mixture of
516 228 tetradecapeptides. Cleavage occurs between P1 and P1′, lowercase "n" is norleucine. **(F**)

Cleavage of internally-quenched fluorescent IL-1β peptide fragments by proteases within BAL collected from C57BL/6 or casp-1/11$^{-/-}$ mice 24 h post-intratracheal infection with 10^7 CFU of PAO1 or Δ*lasB*. Where applicable, data are mean ± SEM and represent at least 3 independent experiments; significance determined by unpaired two-tailed Student's T-test, $*P < 0.05$.

Figure 5. Metalloprotease inhibitors prevent pathological inflammation during *P. aeruginosa* infection

(**A**) Cleavage of internally quenched IL-1β fragment HDAPVRSLN by recombinant LasB incubated with titrations of Marimastat and Ilomastat. (**B**) IL-1 signaling by THP-1 macrophages 2 h post-infection with PAO1, MOI=10, incubated with titrations of Marimastat and Ilomastat. C57BL/6 mice intratracheally infected with 10^7 CFU PAO1 and treated with 25 μg/kg Ilomastat, 25 μg/kg Marimastat, or PBS control. After 24 h, mouse BAL was harvested and (**C**) IL-1β measured by enzyme-linked immunosorbent assay and (**D**) neutrophils enumerated. (**E**) Representative histology sections cytological smears of bronchoalveolar lavage fluid prepared with differential MGG stain. Where applicable, data are mean ± SEM and represent at least 3 independent experiments. Significance determined by Mann-Whitney U-test ($*P < 0.05$, $**P < 0.005$).

Tables and Figures

TABLE 1 Bacterial strains, plasmids, and primers used in this study

Strain, plasmid, or primer	Relevant feature(s) or sequence	Reference or Source
Strains		
P. aeruginosa		
PAO1	WT reference strain	[52]
PAO1 *lasB::Tn*	*lasB* transposon insert	[52]
PAO1 *fliC::Tn*	*fliC* transposon insert	[52]
PAO1 *lasA::Tn*	*lasA* transposon insert	[52]
PAO1 *piv::Tn*	*piv* transposon insert	[52]
PAO1 *lasB::Tn::lasB*	*lasB::Tn* complimented with mTn7T<*lasB*>	This study
MDR-P4	WT strain	G. Sakoulas
PA103	WT strain	ATCC
27312	WT strain	ATCC
27864	WT strain	ATCC
10145	WT strain	ATCC
GNR697	WT strain	G. Sakoulas
Hanity	WT strain	G. Sakoulas
Plasmid		
pET-proIL-1β	Vector for expression of recombinant human pro-IL-1β	[30]
pET-LasB	Vector for expression of recombinant LasB	This study
pUC18T-mTn7T	Complementation vector	[47]
pUC18T<lasB>	*lasB* insertion in mini-Tn7T for complementation	This study
Oligonucleotides		
lasB-F	CAATTCGATCATGCATGAGCTAGCTGCCACCTGCTTTTCT	
lasB-R	CCAAGCTTCTCGAGGAATTCCTTACAACGCGCTCGGG	
pET-LasB-A	TCTGTTCCAGGGGCCCATGAAGAAGGTTTCTACGCTTGAC	
pET-LasB-B	TGCTCGAGTGCGGCCTTACAACGCGCTCGGG	
pET-LasB-C	GTCAAGCGTAGAAACCTTCTTCATGGGCCCCTGGAACAGA	
pET-LasB-D	CCCGAGCGCGTTGTAAGGCCGCACTCGAGCA	
LasB CT His-1	TTGCATCATCATCATCATCACTAAGGCCGCACTCGAGC	
LasB CT His-2	TTAGTGATGATGATGATGATGCAACGCGCTCGGG	
Tn7-F	AGAAAAGCAGGTGGCAGCTAGCTCATGCATGATCGAATT	
Tn7-R	CCCGAGCGCGTTGTAAGGAATTCCTCGAGAAGCTTGG	
il1b-F	TGGACCTTCCAGGATGAGGACA	
il1b-R	GTTCATCTCGGAGCCTGTAGTG	
gapdh-F	TGTGGGCATCAATGGATTTGG	
gapdh-R	ACACCATGTATTCCGGGTCAAT	
IVTTIL1b-term	TTTTTTTTTTTTTTTTTTTTAGGAAGACACAAATTGCATGG	
IVTTIL1b-1	GAAATTAATACGACTCACTATAGGGAGACCCCACCATGGCAGAAGTACCTGAGCTCGC	
IVTTIL1b-12	GAAATTAATACGACTCACTATAGGGAGACCCCACCATGATGGCTTATTACAGTGGCAA	
IVTTIL1b-24	GAAATTAATACGACTCACTATAGGGAGACCCCACCATGTTTGAAGCTGATGGCCCTAA	
IVTTIL1b-36	GAAATTAATACGACTCACTATAGGGAGACCCCACCATGTTCCAGGACCTGGACCTCTG	
IVTTIL1b-48	GAAATTAATACGACTCACTATAGGGAGACCCCACCATGATCCAGCTACGAATCTCCGA	
IVTTIL1b-60	GAAATTAATACGACTCACTATAGGGAGACCCCACCATGGGCTTCAGGCAGGCCGCGTC	
IVTTIL1b-72	GAAATTAATACGACTCACTATAGGGAGACCCCACCATGGACAAGCTGAGGAAGATGCT	
IVTTIL1b-84	GAAATTAATACGACTCACTATAGGGAGACCCCACCATGACCTTCCAGGAGAATGACCT	
IVTTIL1b-87	GAAATTAATACGACTCACTATAGGGAGACCCCACCATGGAGAATGACCTGAGCACCTT	
IVTTIL1b-90	GAAATTAATACGACTCACTATAGGGAGACCCCACCATGCTGAGCACCTTCTTTCCCTT	
IVTTIL1b-93	GAAATTAATACGACTCACTATAGGGAGACCCCACCATGTTCTTTCCCTTCATCTTTGA	
IVTTIL1b-96	GAAATTAATACGACTCACTATAGGGAGACCCCACCATGTTCATCTTTGAAGAAGAACC	
IVTTIL1b-99	GAAATTAATACGACTCACTATAGGGAGACCCCACCATGGAAGAAGAACCTATCTTCTT	
IVTTIL1b-102	GAAATTAATACGACTCACTATAGGGAGACCCCACCATGCCTATCTTCTTCGACACATG	
IVTTIL1b-105	GAAATTAATACGACTCACTATAGGGAGACCCCACCATGTTCGACACATGGGATAACGA	
IVTTIL1b-108	GAAATTAATACGACTCACTATAGGGAGACCCCACCATGTGGGATAACGAGGCTTATGT	
IVTTIL1b-111	GAAATTAATACGACTCACTATAGGGAGACCCCACCATGGAGGCTTATGTGCACGATGC	
IVTTIL1b-114	GAAATTAATACGACTCACTATAGGGAGACCCCACCATGGTACGATCACTGAACTGCACG	
IVTTIL1b-117	GAAATTAATACGACTCACTATAGGGAGACCCCACCATGGCACCTGTACGATCACTGAAC	
IVTTIL1b-120	GAAATTAATACGACTCACTATAGGGAGACCCCACCATGCGATCACTGAACTGCACGCT	
IVTTIL1b-122	GAAATTAATACGACTCACTATAGGGAGACCCCACCATGCTGAACTGCACGCTCCGGGAC	
IVTTIL1b-123	GAAATTAATACGACTCACTATAGGGAGACCCCACCATGAACTGCACGCTCCGGGACTC	
IVTTIL1b-126	GAAATTAATACGACTCACTATAGGGAGACCCCACCATGCTCCGGGACTCACAGCAAAA	

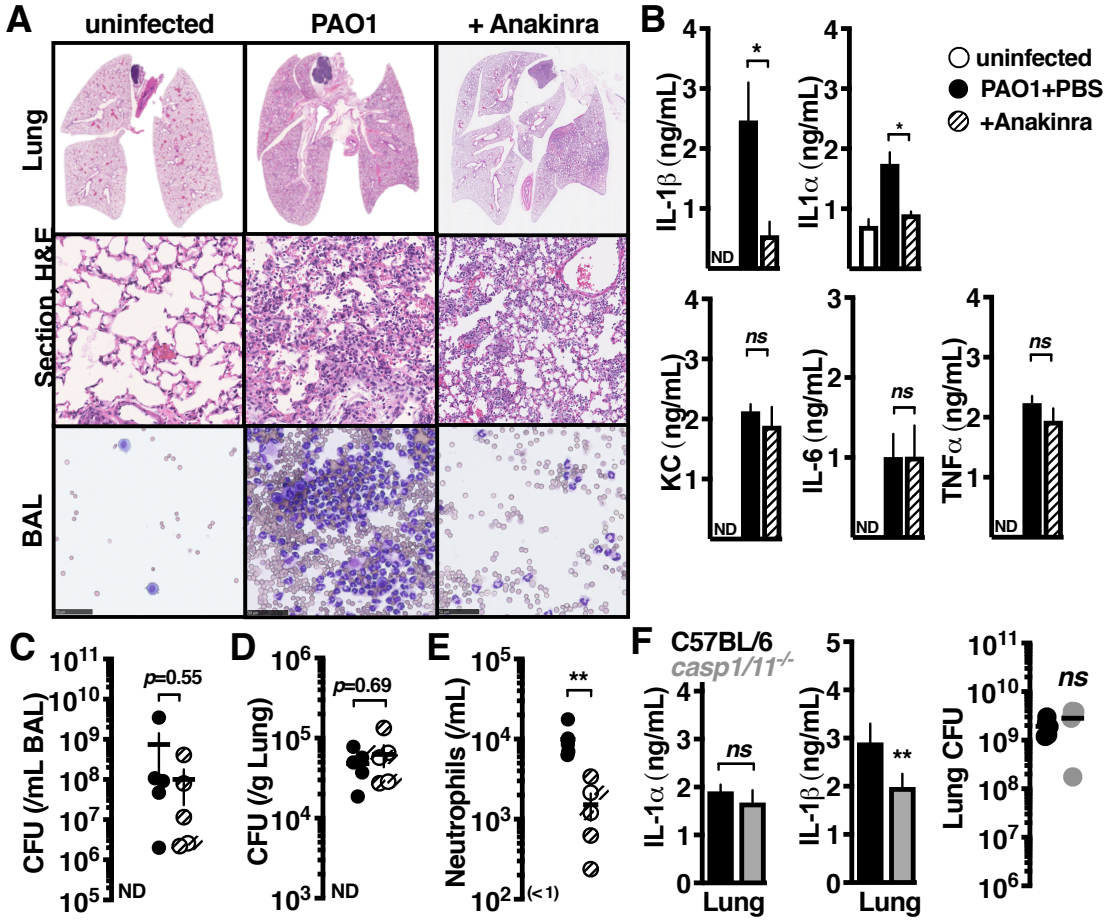
A
uninfected
PAO1
+ Anakinra
Lung
Section, H&E
BAL
B
uninfected
PAO1+PBS
+Anakinra
IL-1β (ng/mL)
IL1α (ng/mL)
KC (ng/mL)
IL-6 (ng/mL)
TNFα (ng/mL)
ND
*
ns
C
CFU (/mL BAL)
p=0.55
ND
D
CFU (/g Lung)
p=0.69
ND
E
Neutrophils (/mL)
**
(<1)
F
C57BL/6
casp1/11-/-
IL-1α (ng/mL)
IL-1β (ng/mL)
Lung CFU
Lung
ns
**

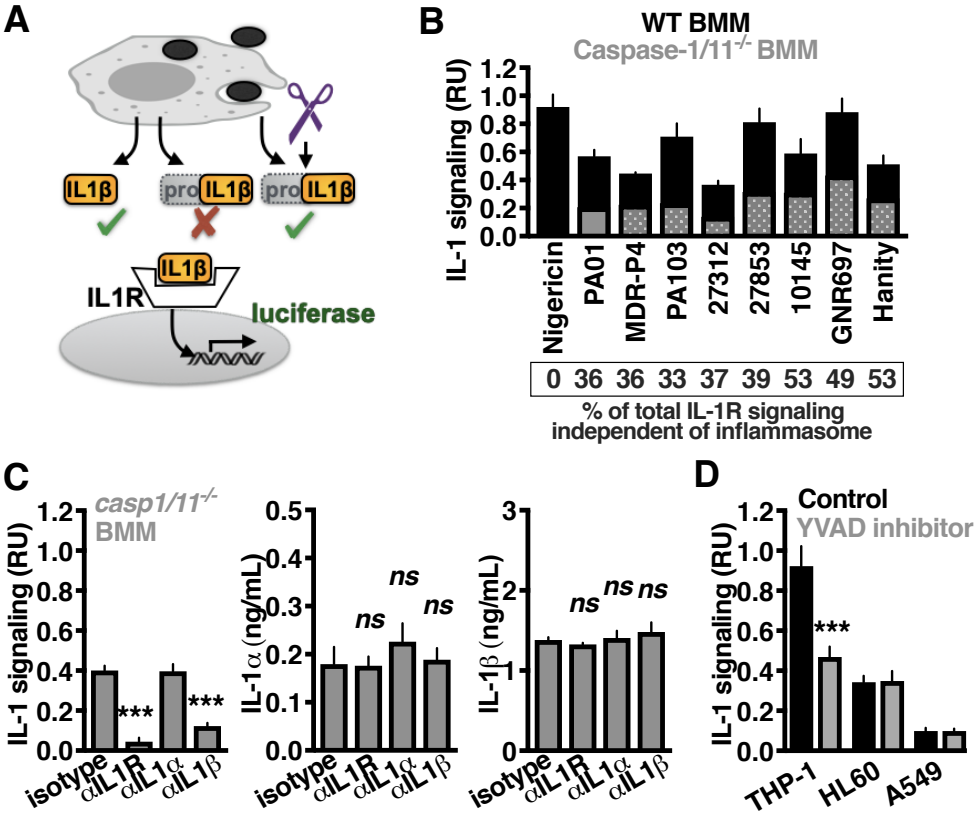
A
IL1β
pro IL1β
pro IL1β
IL1β
IL1R
luciferase
B
WT BMM
Caspase-1/11-/- BMM
IL-1 signaling (RU)
1.2
1.0
0.8
0.6
0.4
0.2
0.0
Nigericin
PA01
MDR-P4
PA103
27312
27853
10145
GNR697
Hanity
0 36 36 33 37 39 53 49 53
% of total IL-1R signaling
independent of inflammasome
C
casp1/11-/-
BMM
IL-1 signaling (RU)
***
***
isotype
αIL1R
αIL1α
αIL1β
IL-1α (ng/mL)
ns
ns
ns
ns
IL-1β (ng/mL)
ns
ns
ns
D
Control
YVAD inhibitor
IL-1 signaling (RU)
***
THP-1
HL60
A549

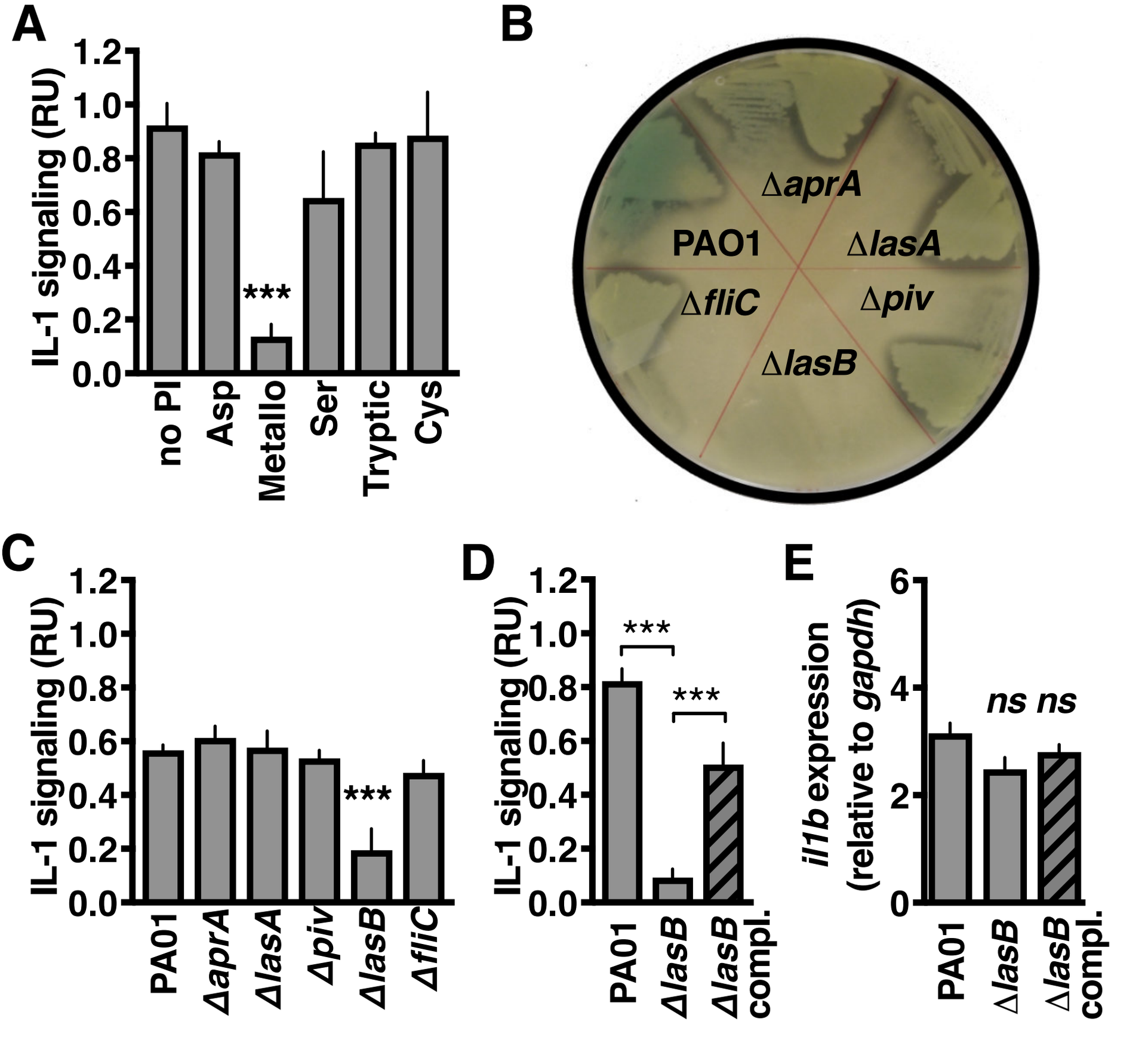
A
IL-1 signaling (RU)
1.2
1.0
0.8
0.6
0.4
0.2
0.0
***
no PI
Asp
Metallo
Ser
Tryptic
Cys
B
ΔaprA
PAO1
ΔlasA
ΔfliC
Δpiv
ΔlasB
C
IL-1 signaling (RU)
1.2
1.0
0.8
0.6
0.4
0.2
0.0
***
PA01
ΔaprA
ΔlasA
Δpiv
ΔlasB
ΔfliC
D
IL-1 signaling (RU)
1.2
1.0
0.8
0.6
0.4
0.2
0.0
***
***
PA01
ΔlasB
ΔlasB compl.
E
il1b expression (relative to gapdh)
6
4
2
0
ns ns
PA01
ΔlasB
ΔlasB compl.

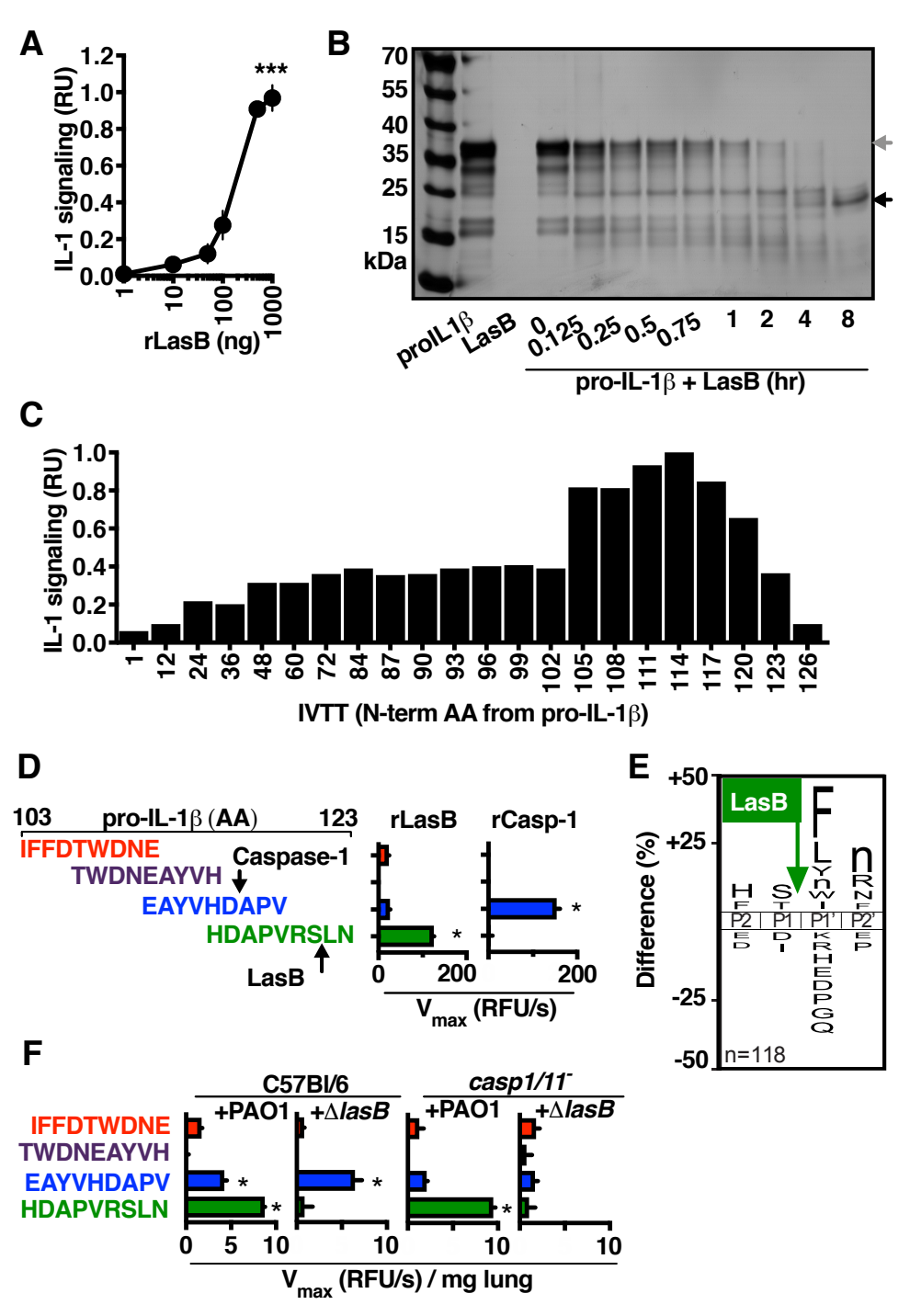
A
IL-1 signaling (RU)
1.2
1.0
0.8
0.6
0.4
0.2
0.0
***
1
10
100
1000
rLasB (ng)
B
70
55
40
35
25
15
kDa
proIL1β
LasB
0
0.125
0.25
0.5
0.75
1
2
4
8
pro-IL-1β + LasB (hr)
C
IL-1 signaling (RU)
1.0
0.8
0.6
0.4
0.2
0.0
1
12
24
36
48
60
72
84
87
90
93
96
99
102
105
108
111
114
117
120
123
126
IVTT (N-term AA from pro-IL-1β)
D
103
pro-IL-1β (AA)
123
IFFDTWDNE
TWDNEAYVH
EAYVHDAPV
HDAPVRSLN
Caspase-1
LasB
rLasB
rCasp-1
0
200
200
Vmax (RFU/s)
E
LasB
+50
+25
-25
-50
Difference (%)
P2
P1
P1'
P2'
n=118
F
C57Bl/6
casp1/11-
+PAO1
+ΔlasB
+PAO1
+ΔlasB
IFFDTWDNE
TWDNEAYVH
EAYVHDAPV
HDAPVRSLN
0
5
10
10
10
10
Vmax (RFU/s) / mg lung

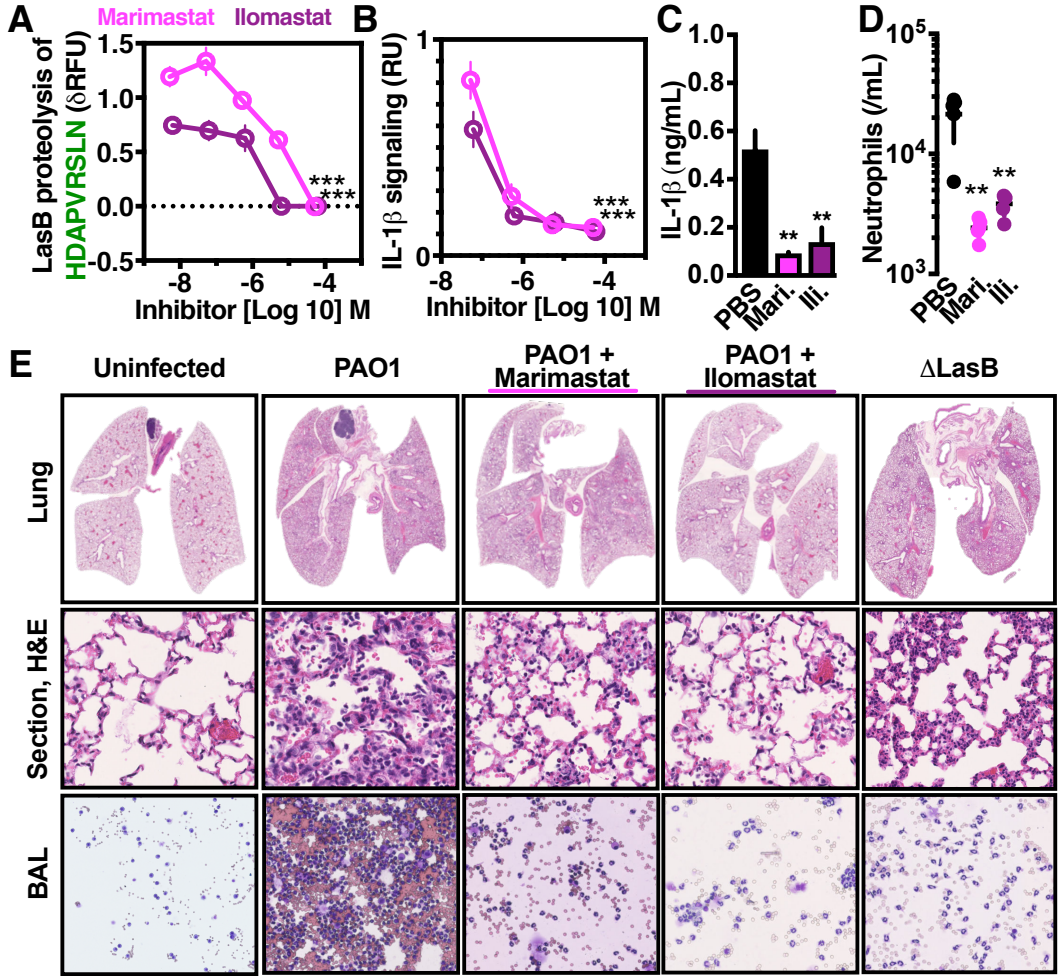
A
Marimastat
Ilomastat
LasB proteolysis of HDAPVRSLN (δRFU)
1.5
1.0
0.5
0.0
-0.5
-8
-6
-4
Inhibitor [Log 10] M
***
***
B
IL-1β signaling (RU)
1
0
-8
-6
-4
Inhibitor [Log 10] M
***
***
C
IL-1β (ng/mL)
1.0
0.8
0.6
0.4
0.2
0.0
**
**
PBS
Mari.
Ili.
D
Neutrophils (/mL)
10^5
10^4
10^3
**
**
PBS
Mari.
Ili.
E
Uninfected
PAO1
PAO1 + Marimastat
PAO1 + Ilomastat
ΔLasB
Lung
Section, H&E
BAL